Article

Global human-made mass exceeds all living biomass

https://doi.org/10.1038/s41586-020-3010-5

Received: 1 November 2019

Accepted: 9 October 2020

Published online: 9 December 2020

Check for updates

Emily Elhacham[1], Liad Ben-Uri[1], Jonathan Grozovski[1], Yinon M. Bar-On[1] & Ron Milo[1]✉

Humanity has become a dominant force in shaping the face of Earth[1–9]. An emerging question is how the overall material output of human activities compares to the overall natural biomass. Here we quantify the human-made mass, referred to as 'anthropogenic mass', and compare it to the overall living biomass on Earth, which currently equals approximately 1.1 teratonnes[10,11]. We find that Earth is exactly at the crossover point; in the year 2020 (± 6), the anthropogenic mass, which has recently doubled roughly every 20 years, will surpass all global living biomass. On average, for each person on the globe, anthropogenic mass equal to more than his or her bodyweight is produced every week. This quantification of the human enterprise gives a mass-based quantitative and symbolic characterization of the human-induced epoch of the Anthropocene.

The face of Earth in the twenty-first century is affected in an unprecedented manner by the activities of humanity and the production and accumulation of human-made objects. Given the limitations of human cognition in the face of the immensity of the globe and the seeming infinity of the natural world, it is desirable to provide a rigorous and objective measure of the overall balance between the living and human-made. However, in spite of pioneering efforts[1–8], we lack a holistic picture that quantifies and compares the composition of the world in terms of both biological and human-made mass.

A case in point is our planet's biomass. While the mass of humans is only about 0.01% of global biomass, our civilization had already had a substantial and diverse impact on it by 3,000 years ago[9]. Since the first agricultural revolution, humanity has roughly halved the mass of plants, from approximately two teratonnes (Tt, units of 10^{12} tonne; where estimates are on a dry-mass basis) down to the current value[10] of approximately 1 Tt. While modern agriculture utilizes an increasing land area for growing crops, the total mass of domesticated crops (about 0.01 Tt)[11] is vastly outweighed by the loss of plant mass resulting from deforestation, forest management and other land-use changes[10]. These trends in global biomass have affected the carbon cycle and human health[12,13]. Additional human actions, including livestock husbandry, hunting and overfishing, have also strongly affected the masses of various other taxa[11,14,15]. A recent survey of Earth's remaining living biomass[11] has found that, on a mass basis, plants constitute the vast majority (about 90%)[16], followed by bacteria, fungi, archaea, protists, and animals.

Beyond biomass, as the global effect of humanity accelerates, it is becoming ever more imperative to quantitatively assess and monitor the material flows of our socioeconomic system, also known as the socioeconomic metabolism[17,18]. This quantification is at the heart of the economy-wide material flow analysis framework, under the field of industrial ecology, which is based on mass balance accounting[19,20]. This extensively developed framework enables researchers to investigate the material basis of society, on local and global scales. It includes the mass and composition of socioeconomic material stocks as well as input and output material flows. A recent study used and expanded the framework to quantify global values for the human-made mass flows and standing stocks[21,22] (objects that have been built by humans and are still in use: buildings, roads, machines and so on).

These advances in the global quantification of both living biomass and human-made mass provide an opportunity to conduct an integrated comparison of the two, which is the primary focus of this paper. Comparing biomass with human-made mass necessitates bringing together objects with different attributes, going beyond comparing apples and oranges to compare apples and mobile phones. However, we find that because living biomass surrounds and supports humanity, it is a natural logical reference point to give a quantitative perspective on the mass that humanity has produced. By contrasting human-made mass and biomass over time, we present an additional dimension to the ongoing assessment of the evolving human dominance on Earth and provide a visual and symbolic characterization of the Anthropocene.

We estimate the global biomass and human-made mass from 1900 in units of teratonnes (which equal 10^{18} grams) of dry weight (that is, excluding water). Biomass represents the overall global mass of all living taxa[11]. Anthropogenic mass is defined as the mass embedded in inanimate solid objects made by humans (that have not been demolished or taken out of service, which we define as 'anthropogenic mass waste'). The mass of humans themselves (and their livestock) is naturally accounted for as part of the global biomass. In any case their mass contribution is negligible. Figure 1 shows changes in biomass and anthropogenic mass over the studied period. It is clear that the two exhibit markedly different temporal dynamics. Over the past 100 years, anthropogenic mass has increased rapidly—doubling in a Moore-law-like fashion approximately every 20 years—in contrast to total biomass, which has not changed as markedly (affected by a complex interplay of deforestation, afforestation and the rising CO_2 fertilization effect, among other things). The accumulation of anthropogenic mass has now reached 30 Gt per year, based on the average for the past 5 years. This corresponds to each person on the globe producing more than his or her body weight in anthropogenic mass every

[1]Department of Plant and Environmental Sciences, Weizmann Institute of Science, Rehovot, Israel. ✉e-mail: ron.milo@weizmann.ac.il

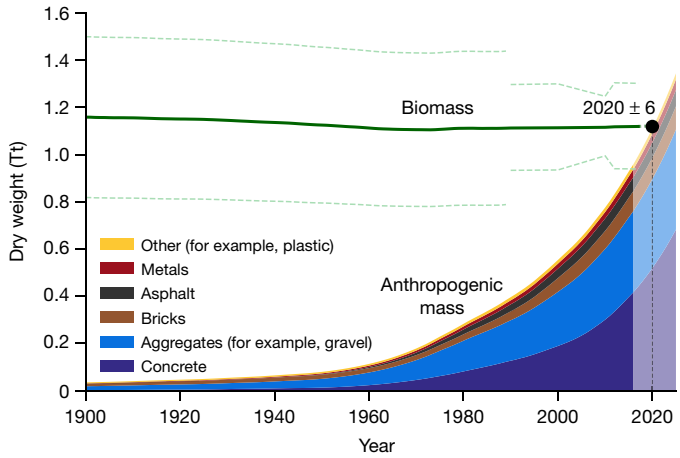

Fig. 1 | Biomass and anthropogenic mass estimates since the beginning of the twentieth century on a dry-mass basis. The green line shows the total weight of the biomass (dashed green lines, ±1 s.d.). Anthropogenic mass weight is plotted as an area chart, where the heights of the coloured areas represent the mass of the corresponding category accumulated until that year. The anthropogenic mass presented here is grouped into six major categories. The year 2020 ± 6 marks the time at which biomass is exceeded by anthropogenic mass. Anthropogenic mass data since 1900 were obtained from ref. [22], at a single-year resolution. The current biomass value is based on ref. [11], which for plants relies on the estimate of ref. [10], which updates earlier, mostly higher estimates. The uncertainty of the year of intersection was derived using a Monte Carlo simulation, with 10,000 repeats (see Methods). Data were extrapolated for the years 2015–2025 (lighter area; see Methods). For a detailed view of the stock accumulation for the 'metals' and 'other' groups, see Extended Data Figs. 4, 5.

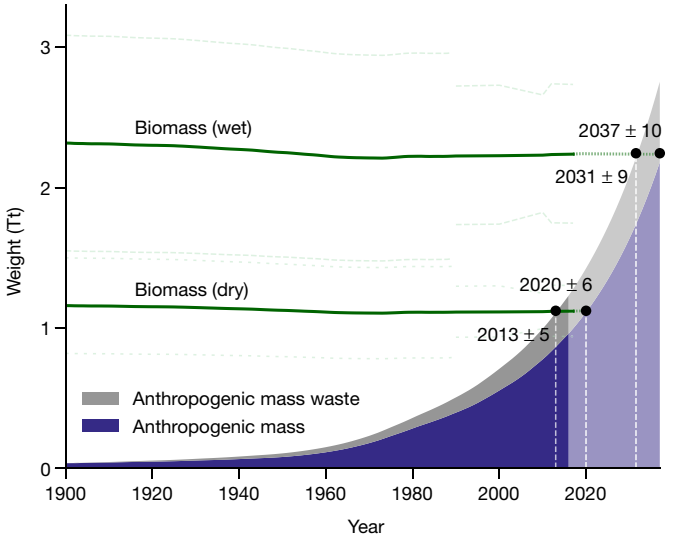

Fig. 2 | Biomass (dry and wet), anthropogenic mass and anthropogenic mass waste estimates since the beginning of the twentieth century. Green lines show the total weight of biomass (±1 s.d.). Anthropogenic mass weight is plotted as an area chart. The wet-weight estimate is based on the results presented in Fig. 1 and the respective water content of major components (see Methods). The year 2013 ± 5 marks the time at which the dry biomass is exceeded by the anthropogenic mass, including waste. The years 2037 ± 10 and 2031 ± 9 mark the times at which the wet biomass is exceeded by the anthropogenic mass and the total produced anthropogenic mass, respectively. The uncertainties of the years of intersection were derived using a Monte Carlo simulation, with 10,000 repeats (see Methods). Weights are extrapolated for the years 2015–2037 (lighter area; see Methods).

week. As a result, the gap between anthropogenic mass and overall biomass has quickly shrunk. We find that the two curves intersect in the year 2020 ± 6 years (1 s.d.), at which point anthropogenic mass will surpass biomass.

The anthropogenic mass is divided into sub-groups, which constitute human-made objects[22] (Extended Data Table 1): concrete, aggregates, bricks, asphalt, metals and 'other' components (wood used for paper and industry, glass and plastic). As shown in Fig. 1, the anthropogenic mass is dominated by concrete and aggregates (such as gravel). The crossover year has an uncertainty that arises from an uncertainty of ±16% for overall biomass and ±6% for anthropogenic mass, with all uncertainties reported as ±1 s.d. The analysis shown in Fig. 1 presents biomass on a dry-weight basis. To provide a complementary point of view, Fig. 2 shows biomass on a wet-mass basis and compares it to anthropogenic mass and accumulated anthropogenic mass waste. Anthropogenic mass waste is anthropogenic mass that has been demolished or taken out of service (time-integrated cumulative solid waste flow, subsequently referred to as simply 'waste'. This does not include unused mass excavated through mining, landscape modification and so on). When we include the waste component, dry biomass is surpassed at 2013 (± 5 years). On a wet-weight basis, the current biomass stands at approximately 2.2 Tt and is expected to be exceeded by anthropogenic mass by the 2030s, with (2031 ± 9 years) or without (2037 ± 10 years) the inclusion of waste. A sensitivity analysis of the effect of the anthropogenic mass definition on the intersection year is presented in Extended Data Fig. 1 and detailed in Supplementary Information section 1.

Figure 3 shows some key relations between major human-made and biological entities. The two dominant mass categories in our analysis are buildings and infrastructure (composed of concrete, aggregates, bricks and asphalt) and trees and shrubs (the majority of plant mass and, therefore, of the overall biomass). We find that the former has recently outweighed the latter. Similarly, we show that the global mass of produced plastic is greater than the overall mass of all terrestrial and marine animals combined.

Discussion

At the beginning of the twentieth century, anthropogenic mass was equal to only 3% of global biomass, with a massive difference of about 1.1 Tt on a dry-weight basis. About 120 years later, in 2020, anthropogenic mass is exceeding overall biomass in the world. As shown above, the exact timing of the point at which anthropogenic mass surpasses living biomass is sensitive to the definitions of biomass and anthropogenic mass; for example, whether they are defined on a wet- or dry-mass basis. However, we find that under a range of definitions, the point of transition is in either the past decade or the next two (Supplementary Information section 1, Extended Data Fig. 1).

The analysis of the changes in anthropogenic mass composition across the studied period highlights specific trends (Extended Data Fig. 2). For example, the gradual shift from construction dominated by bricks to concrete, which tilted in favour of concrete in the mid-1950s, is clear, as is the emergence of asphalt as a major road pavement material from the 1960s. Analysis of the rate of accumulation of anthropogenic mass further provides a material-based view of humanity's path since the beginning of the twentieth century, as shown in Extended Data Fig. 3. Shifts in total anthropogenic mass are tied to global events, such as world wars and major economic crises. Most notably, continuous increases in anthropogenic mass, peaking at over 5% per year, mark the period immediately following World War II. This period, frequently termed the 'Great Acceleration', is characterized by enhanced consumption and urban development[23]. If current trends continue, anthropogenic mass, including waste, is expected to exceed 3 Tt by 2040—almost triple the dry biomass on Earth.

Fig. 3 | Contrasting key components of global biomass and anthropogenic mass in the year 2020 (dry-weight basis). The ratio between the circle areas within each pair represents the corresponding mass ratio of the two illustrated masses. For visual clarity, the two pairs use different scales. The plastic estimate includes plastic currently in use and plastic waste, taking into account recycling. Infrastructure includes the mass of constructed elements, such as roads.

Previous efforts, such as quantifying the human appropriation of net primary production[24–26], have focused on the allocation of the biosphere productivity flow for human usage. The anthropogenic mass, the accumulation of which is documented in this study, does not arise out of the biomass stock but from the transformation of the orders-of-magnitude higher stock of mostly rocks and minerals. In doing so, humanity is converting near-surface geological deposits into a socially useful form, with wide implications for natural habitats, biodiversity, and various climatic and biogeochemical cycles.

This study joins recent efforts to quantify and evaluate the scale and impact of human activities on our planet[9,23,27,28]. The impacts of these activities have been so abrupt and considerable that it has been proposed that the current geological epoch be renamed the Anthropocene[29–32]. Our study rigorously and quantitatively substantiates this proposal. In parallel, it adds another dimension to this discussion—a symbolic quantitative demarcation of the transition to our epoch.

Online content

Any methods, additional references, Nature Research reporting summaries, source data, extended data, supplementary information, acknowledgements, peer review information; details of author contributions and competing interests; and statements of data and code availability are available at https://doi.org/10.1038/s41586-020-3010-5.

1. Ramankutty, N. & Foley, J. A. Estimating historical changes in global land cover: croplands from 1700 to 1992. *Glob. Biogeochem. Cycles* **13**, 997–1027 (1999).
2. Krausmann, F. et al. Growth in global materials use, GDP and population during the 20th century. *Ecol. Econ.* **68**, 2696–2705 (2009).
3. Matthews, E. *The Weight of Nations: Material Outflows from Industrial Economies* (World Resources Inst., 2000).
4. Smil, V. *Harvesting the Biosphere: What We Have Taken from Nature* (MIT Press, 2013).
5. Smil, V. *Making the Modern World: Materials and Dematerialization* (John Wiley & Sons, 2013).
6. Haff, P. K. Technology as a geological phenomenon: implications for human well-being. *Geol. Soc. Lond. Spec. Publ.* **395**, 301–309 (2014).
7. Zalasiewicz, J. et al. Scale and diversity of the physical technosphere: a geological perspective. *Anthropocene Rev.* **4**, 9–22 (2017).
8. Zalasiewicz, J., Waters, C. N., Williams, M. & Summerhayes, C. *The Anthropocene as a Geological Time Unit: A Guide to the Scientific Evidence and Current Debate* (Cambridge Univ. Press, 2018).
9. Stephens, L. et al. Archaeological assessment reveals Earth's early transformation through land use. *Science* **365**, 897–902 (2019).
10. Erb, K.-H. et al. Unexpectedly large impact of forest management and grazing on global vegetation biomass. *Nature* **553**, 73–76 (2018).
11. Bar-On, Y. M., Phillips, R. & Milo, R. The biomass distribution on Earth. *Proc. Natl Acad. Sci. USA* **115**, 6506–6511 (2018).
12. Pan, Y. et al. A large and persistent carbon sink in the world's forests. *Science* **333**, 988–993 (2011).
13. Reddington, C. L. et al. Air quality and human health improvements from reductions in deforestation-related fire in Brazil. *Nat. Geosci.* **8**, 768–771 (2015).
14. Ceballos, G. & Ehrlich, P. R. Mammal population losses and the extinction crisis. *Science* **296**, 904–907 (2002).
15. WWF. *Living Planet Report–2018: Aiming Higher* (WWF, 2018).
16. Bar-On, Y. M. & Milo, R. Towards a quantitative view of the global ubiquity of biofilms. *Nat. Rev. Microbiol.* **17**, 199–200 (2019).
17. Pauliuk, S. & Hertwich, E. G. Socioeconomic metabolism as paradigm for studying the biophysical basis of human societies. *Ecol. Econ.* **119**, 83–93 (2015).
18. Haberl, H. et al. Contributions of sociometabolic research to sustainability science. *Nat. Sustainability* **2**, 173–184 (2019).
19. Fischer-Kowalski, M. et al. Methodology and indicators of economy-wide material flow accounting. *J. Ind. Ecol.* **15**, 855–876 (2011).
20. Krausmann, F., Schandl, H., Eisenmenger, N., Giljum, S. & Jackson, T. Material flow accounting: measuring global material use for sustainable development. *Annu. Rev. Environ. Resour.* **42**, 647–675 (2017).
21. Krausmann, F. et al. Global socioeconomic material stocks rise 23-fold over the 20th century and require half of annual resource use. *Proc. Natl Acad. Sci. USA* **114**, 1880–1885 (2017).
22. Krausmann, F., Lauk, C., Haas, W. & Wiedenhofer, D. From resource extraction to outflows of wastes and emissions: the socioeconomic metabolism of the global economy, 1900–2015. *Glob. Environ. Change* **52**, 131–140 (2018).
23. Steffen, W., Broadgate, W., Deutsch, L., Gaffney, O. & Ludwig, C. The trajectory of the Anthropocene: the great acceleration. *Anthropocene Rev.* **2**, 81–98 (2015).
24. Vitousek, P. M., Ehrlich, P. R., Ehrlich, A. H. & Matson, P. A. Human appropriation of the products of photosynthesis. *Bioscience* **36**, 368–373 (1986).
25. Haberl, H. et al. Quantifying and mapping the human appropriation of net primary production in Earth's terrestrial ecosystems. *Proc. Natl Acad. Sci. USA* **104**, 12942–12947 (2007).
26. Haberl, H., Erb, K.-H. & Krausmann, F. Human appropriation of net primary production: patterns, trends, and planetary boundaries. *Annu. Rev. Environ. Resour.* **39**, 363–391 (2014).
27. Vitousek, P. M. Human domination of Earth's ecosystems. *Science* **277**, 494–499 (1997).
28. Dirzo, R. et al. Defaunation in the Anthropocene. *Science* **345**, 401–406 (2014).
29. Crutzen, P. J. in *Earth System Science in the Anthropocene* (eds. Ehlers, E. & Kraft, T.) 13–18 (Springer, 2006).
30. Steffen, W., Crutzen, J. & McNeill, J. R. The Anthropocene: are humans now overwhelming the great forces of Nature? *Ambio* **36**, 614–621 (2007).
31. Lewis, S. L. & Maslin, M. A. Defining the Anthropocene. *Nature* **519**, 171–180 (2015).
32. Waters, C. N. et al. The Anthropocene is functionally and stratigraphically distinct from the Holocene. *Science* **351**, aad2622 (2016).

Methods

Anthropogenic mass definition

Our definition of human-made mass, termed here anthropogenic mass, is the mass embedded in inanimate solid objects made by humans (that have not yet been demolished or taken out of service). It originates from material flows from the natural environment to the socioeconomic system, accumulated into stocks of artefacts, also known as manufactured capital[22]. The anthropogenic mass is the visible inanimate component of what has been termed the physical technosphere[6,7]. As biological components of the physical technosphere, including croplands (for example, rice and hay fields, which produce flows to the socioeconomic system[33]) and livestock (part of the socioeconomic system), are living natural biological entities, we classified them under biomass, even though they serve human purposes. Conversely, industrial wood, used in construction, was classified under anthropogenic mass, because it is embedded in human-made artefacts. A similar approach for accounting human-made mass is presented in chapter 1 of ref. [5]. A sensitivity analysis of the anthropogenic mass definition and its effect on the year of intersection is included in Supplementary Information section 1 and Extended Data Fig. 1, as well as at https://anthropomass.org/analysis/.

The anthropogenic mass was divided into six sub-groups: concrete, aggregates, bricks, asphalt, metals and an additional group of other components consisting of wood, glass and plastic. The aggregates group includes the gravel and sand that serve as bedding for roads and buildings. The mass of aggregates incorporated in concrete and asphalt is separately accounted for in the concrete and asphalt categories[21,22,34]. While for some material flows no data are available or could be estimated, overall, the categories of anthropogenic mass presented here give almost complete coverage of materials usage (more than 98% in terms of mass[21]). As customary in material-flow-analysis, the current estimates of flows[22] do not include extracted material not designated for future utilization (for example, "soil and rock excavated during construction or overburden from mining and the unused parts of fellings in forestry"[33]). Sediment movements due to dredging were likewise not included in the estimate[35].

To evaluate the anthropogenic mass waste, the mass flows of end-of-life waste were integrated over time. The waste is accounted from 1900 only, owing to data availability. The anthropogenic mass wood waste, originating from industrial wood and paper[21], is not included in the waste estimate because wood decomposes relatively rapidly. Additional waste groups (representing output flows such as emissions, dissipative use and tailings) were not included in our calculation as they do not represent physical and visible elements and are not part of our definition of anthropogenic mass. Following ref. [22], we also treated controlled landfills as part of the output waste flow. Our waste mass estimates are after deduction of recycling processes. Incineration (that is, energy generation from the combustion of waste) was not included, which results in a small (approximately 2%) overestimation of the waste[22]. Infrastructure that is no longer in service, also known as 'hibernating stocks' (for example, abandoned buildings), was classified under waste.

Anthropogenic mass data since 1900 were obtained from ref. [22] at a single-year resolution. The anthropogenic mass weight was accounted without hydrated water following the standards defined in material flow analysis[21]. The anthropogenic mass starting value at the year 1900 was estimated at about 35 Gt. This value was calculated according to material flow estimates obtained for the time period of 1820–1900 (as described in the Supplementary Information for ref. [21]). We note that estimates from before 1820 are not included, and therefore we assume that the anthropogenic mass value starts from zero at that time. While this is clearly a simplification, accumulated anthropogenic mass until that time will result in a relatively small mass, which will have a negligible contribution to the overall figure for the twentieth century onward.

Biomass change over the years 1900–2017

There have been various previous efforts to quantify global biomass using different methodologies, including inventory assessments[12,36], remote sensing[37] and modelling[38,39]. In our estimate, we sought to synthesize estimates generated by these different approaches. We first estimated plant biomass, which represents about 90% of global biomass[11]. Note that soil carbon is not living biomass and thus is not included in this study.

Plant biomass estimate for the years 1990–2017. Our plant biomass value for 2010, about 0.45 Tt carbon, is based on ref. [11], which relies on the estimate by ref. [10], which consists of the mean of seven maps of global plant biomass that are based on inventories or remote sensing. The estimate of about 0.45 Tt carbon, which updates previous, mostly higher, estimates, has been substantiated as the current gold standard in ref. [10], which extensively surveyed and integrated different estimates and approaches.

To estimate the total plant biomass between 1990 and 2017, we relied on two approaches. The first approach is based on three main data sources, using inventory measurements[12,36,40] or remote sensing[37]. The second is an ensemble of 15 dynamic global vegetation models. To generate our best estimate for total plant biomass, we first calculated a best estimate for each approach by taking the average of all the sources within the same approach and then taking the average of the best estimates produced by each of the two approaches.

Within the period 1990–2017, we used plant biomass estimates at five time points (1990, 2000, 2010, 2012 and 2017), chosen according to data availability (for ref. [12] we used the 2007 estimate; for ref. [37] we used the 1993 estimate). We first normalized the estimates of the different sources in relation to our 2010 estimate, according to the plant biomass component each source includes (either all plants, or forests only, assuming the forest fraction remains constant). Next, for each time point, we took the mean of the normalized biomass estimates across the different sources, to obtain the biomass estimate for each of the time points, as shown in Extended Data Fig. 6.

Our second estimate was based on the normalized mean of 15 state-of-the-art Dynamic Global Vegetation Models (DGVMs; see below). For each of the five selected time points, the obtained estimate was averaged with the inventory and remote sensing-based estimate to result in the plant biomass estimates used in this study.

Plant biomass estimate for the years 1900–1990. The 1900–1990 estimates rely on the 15 DGVMs ensemble annual mean, which was normalized according to our 1990 estimate, calculated as described above.

Non-plant biomass estimate. The non-plant estimate was derived according to a recent global census[11], with new updates for the biomass of bacteria and archaea kingdoms[16,41]. The updates included a decrease in the overall mass of bacteria and archaea, from about 0.08 to about 0.03 Tt carbon. For lack of better information, the non-plant estimate was assumed to remain constant throughout the studied period. As it is an order of magnitude less than the plant biomass, any missing temporal changes in non-plant biomass are expected to have only minor quantitative overall effects on our analysis.

Overall biomass estimates. As a final step, the non-plant biomass was added to the plant biomass. The sums were multiplied by a carbon-weight-to-dry-weight factor (as discussed in the 'Biomass C content estimation' section), to obtain the biomass estimates presented in this study.

All the steps from raw data to end results are documented in a Jupyter notebook available at https://github.com/milo-lab/anthropogenic_mass/tree/master/biomass_calculation/biomass_calculation.ipynb.

Dynamic global vegetation models

DGVM outputs were used in our plant biomass estimates throughout the studied period. For the years 1990–2017, the estimates were integrated with non-model estimates, as described above. The simulation outputs are part of the TRENDY v.8 project[38,39], and followed the same protocol, including both land-use and environmental (climate, CO_2) time-varying effects (denoted as S3 in TRENDY; see ref. [39] and https://sites.exeter.ac.uk/trendy for further details). The ensemble used here comprised the following 15 models: CABLE-POP[42], CLASS-CTEM[43], CLM5.0[44], DLEM[45], ISAM[46], JSBACH[47], JULES-ES[48], LPJ[49], LPJ-GUESS[50], LPX-Bern[51], OCN[52], ORCHIDEE[53], ORCHIDEE-CNP[54], SDGVM[55] and VISIT[56].

Anthropogenic mass and biomass extrapolation

Extrapolation was used to estimate the time of intersection in Fig. 2 for the wet weight of biomass. To derive the future biomass change (2018–2037), we used the linear rate of change calculated for 2010–2017, and assumed that it would remain constant. The overall trend was found to be almost neutral given the uncertainty, as further discussed in Supplementary Information section 2. Anthropogenic mass estimates for future years (2015–2037) were extrapolated under an exponential growth scenario. The exponent was derived on the basis of the most recent 5 years for which data were available[22], under the simplified assumption that it would remain constant.

Biomass C content estimation

As part of the biomass calculation, we converted biomass on a carbon-weight basis to a dry-weight basis by multiplying by a conversion factor (2.25 g/g), which was calculated from estimates of the C content of different plant compartments (leaves, stems and roots) differentiated by biome[57]. For each biome, we calculated the average plant C content according to the mass fraction of each plant compartment[58]. Subsequently, the overall weighted plant C content was calculated on the basis of the corresponding mass fraction of each biome[10].

The total biomass C content conversion factor was then derived by computing the weighted average of the plant and non-plant factors, assuming that non-plant biomass represents 10% of total biomass (based on ref. [11] and updates[16,41]). C content estimates for bacteria, which represent the major contributor to non-plant biomass, were obtained from refs. [59,60]. All steps from raw data to end result are documented in a Jupyter notebook available at https://github.com/milo-lab/anthropogenic_mass/tree/master/C_content/biomass_C_content_estimation.ipynb.

Biomass wet-weight estimation

The biomass wet-weight was evaluated using a wet-to-dry-mass conversion factor (M_{wet}/M_{dry}, the ratio between the wet and dry weights). The factor is composed of the corresponding factors of the main three tree compartments: roots, stems and leaves.

The roots' conversion factor was calculated according to 30 wet-to-dry root mass measurements of four tree species[61]. Our best estimate for the conversion factor, 2.1 g/g, was the geometric mean of all calculated conversion factors of all samples.

The stems' conversion factor was computed using a dataset of the average green wood moisture content ($(M_{wet} - M_{dry})/M_{dry}$) of 62 tree species[62]. The dataset contains the moisture content values of sapwood and heartwood for each species. The best estimate of each species' moisture content value was based on the mean of the respective sapwood and heartwood moisture content values (assuming a 1:1 mass ratio between heartwood and sapwood). We then converted all moisture content values to wet-to-dry-mass conversion factors. The geometric mean of the corresponding factors of all species was found to be 1.9 and was used as our best estimate.

The conversion factor of leaves was derived from dry matter content (M_{dry}/M_{wet}) datasets[63–68], including 218 plant species, obtained via TryDB[69]. For each species, the geometric mean dry matter content value was calculated. Our best estimate of the leaves' dry matter content was the geometric mean of all values. It was found to be 0.33 g/g, and thus the wet-to-dry-mass conversion factor we used was 1/0.33 = 3.0.

The three conversion factors were then multiplied by their corresponding compartment global dry mass[11] to yield the global compartment wet mass. Those were summed together to obtain the overall global plant wet mass. We later combined the three factors to generate a single integrated conversion factor, by dividing the global plant wet mass by the dry mass. This integrated factor (2.0 g/g) was used throughout this study to derive the overall biomass wet mass according to the dry mass. All steps from raw data to end result are documented in a Jupyter notebook at https://github.com/milo-lab/anthropogenic_mass/tree/master/wet_weight_calculation/wet_weight_calculation.ipynb.

Uncertainty estimation

Error propagation was performed using the Python Uncertainties Package[70]. The carbon-to-dry-weight conversion factor was derived according to C content estimates obtained from different biomes (see 'Biomass C content estimation' section). The overall uncertainty was found to be ±6%. The wet-to-dry conversion factor was calculated using values measured separately for roots, stems and leaves (see 'Biomass wet-weight estimation' section). We found the total uncertainty of the dry-to-wet-weight conversion factor to be ±15%.

The uncertainties of the years in which the anthropogenic mass and biomass intersect were estimated using Monte Carlo simulations, with each parameter (for example, for dry biomass and wet-to-dry-conversion-factor) randomly drawn according to its uncertainty range. The process was repeated 10,000 times, with the resulting distribution dictating the overall uncertainty. All uncertainties are reported as ±1 s.d. The anthropogenic mass uncertainties used were based on corresponding estimates from ref. [22], assuming a normal distribution. The uncertainties of the anthropogenic mass vary from ±2% to ±6% across the studied period. The waste uncertainties range from ±4% in 1900 to ±7% in 2015. All calculation steps are documented in a Jupyter notebook at https://github.com/milo-lab/anthropogenic_mass/tree/master/intersection_year_uncertainty/intersection_year_uncertainty.ipynb.

Following the biomass calculation (as described in the 'Biomass change over the years 1900–2017' section), the total dry biomass uncertainty was found to be ±16% for the years after 1990, and ±29% for earlier years (±22% and ±33% for a wet-weight basis). The uncertainty was derived using the Python Uncertainties Package for the plant component, Monte Carlo simulations for the non-plant component, and propagation[70]. All calculation steps are documented in a Jupyter notebook at https://github.com/milo-lab/anthropogenic_mass/tree/master/biomass_calculation/biomass_uncertainty.ipynb.

Reporting summary

Further information on research design is available in the Nature Research Reporting Summary linked to this paper.

Data availability

All data used in this study are available on GitHub, at https://github.com/milo-lab/anthropogenic_mass. Anthropogenic mass data are available from ref. [22] and at https://boku.ac.at/wiso/sec/data-download. TRENDY Dynamic Global Vegetation Models outputs are available at https://sites.exeter.ac.uk/trendy. Leaves dry matter content measurements were obtained via TryDB, at https://www.try-db.org/. Other datasets used in this study are available from the published literature, as detailed in the Methods and Supplementary Information.

Code availability

All code used in this study is available on GitHub, at https://github.com/milo-lab/anthropogenic_mass.

33. Krausmann, F. *et al*. *Economy-wide Material Flow Accounting. Introduction and Guide* Version 1, Social Ecology Working Paper 151 (Alpen-Adria Univ., 2015).
34. Miatto, A., Schandl, H., Fishman, T. & Tanikawa, H. Global patterns and trends for non-metallic minerals used for construction. *J. Ind. Ecol*. **21**, 924–937 (2017).
35. Cooper, A. H., Brown, T. J., Price, S. J., Ford, J. R. & Waters, C. N. Humans are the most significant global geomorphological driving force of the 21st century. *Anthropocene Rev*. **5**, 222–229 (2018).
36. Food and Agriculture Organization of the United Nations. *Global Forest Resources Assessment 2010: Main Report* (FAO, 2010).
37. Liu, Y. Y. et al. Recent reversal in loss of global terrestrial biomass. *Nat. Clim. Chang*. **5**, 470–474 (2015).
38. Sitch, S. et al. Recent trends and drivers of regional sources and sinks of carbon dioxide. *Biogeosciences* **12**, 653–679 (2015).
39. Friedlingstein, P. et al. Global carbon budget 2019. *Earth Syst. Sci. Data* **11**, 1783–1838 (2019).
40. Food and Agriculture Organization of the United Nations *FAOSTAT* http://faostat.fao.org.
41. Magnabosco, C. et al. The biomass and biodiversity of the continental subsurface. *Nat. Geosci*. **11**, 707–717 (2018).
42. Haverd, V. et al. A new version of the CABLE land surface model (Subversion revision r4601) incorporating land use and land cover change, woody vegetation demography, and a novel optimisation-based approach to plant coordination of photosynthesis. *Geosci. Model Dev*. **11**, 2995–3026 (2018).
43. Melton, J. R. & Arora, V. K. Competition between plant functional types in the Canadian Terrestrial Ecosystem Model (CTEM) v. 2.0. *Geosci. Model Dev*. **9**, 323–361 (2016).
44. Lawrence, D. M. et al. The community land model version 5: description of new features, benchmarking, and impact of forcing uncertainty. *J. Adv. Model. Earth Syst*. **11**, 4245–4287 (2019).
45. Tian, H. et al. North American terrestrial CO_2 uptake largely offset by CH_4 and N_2O emissions: toward a full accounting of the greenhouse gas budget. *Clim. Change* **129**, 413–426 (2015).
46. Meiyappan, P., Jain, A. K. & House, J. I. Increased influence of nitrogen limitation on CO_2 emissions from future land use and land use change. *Glob. Biogeochem. Cycles* **29**, 1524–1548 (2015).
47. Mauritsen, T. et al. Developments in the MPI-M Earth System Model version1.2 (MPI-ESM1.2) and its response to increasing CO_2. *J. Adv. Model. Earth Syst*. **11**, 998–1038 (2019).
48. Clark, D. B. et al. The Joint UK Land Environment Simulator (JULES), model description – Part 2: Carbon fluxes and vegetation dynamics. *Geosci. Model Dev*. **4**, 701–722 (2011).
49. Poulter, B., Frank, D. C., Hodson, E. L. & Zimmermann, N. E. Impacts of land cover and climate data selection on understanding terrestrial carbon dynamics and the CO_2 airborne fraction. *Biogeosciences* **8**, 2027–2036 (2011).
50. Smith, B. et al. Implications of incorporating N cycling and N limitations on primary production in an individual-based dynamic vegetation model. *Biogeosciences* **11**, 2027–2054 (2014).
51. Lienert, S. & Joos, F. A Bayesian ensemble data assimilation to constrain model parameters and land-use carbon emissions. *Biogeosciences* **15**, 2909–2930 (2018).
52. Zaehle, S. & Friend, A. D. Carbon and nitrogen cycle dynamics in the O-CN land surface model: 1. Model description, site-scale evaluation, and sensitivity to parameter estimates. *Glob. Biogeochem. Cycles* **24**, GB1005 (2010).
53. Krinner, G. et al. A dynamic global vegetation model for studies of the coupled atmosphere–biosphere system. *Glob. Biogeochem. Cycles* **19**, GB1015 (2005).
54. Goll, D. S. et al. Carbon–nitrogen interactions in idealized simulations with JSBACH (version 3.10). *Geosci. Model Dev*. **10**, 2009–2030 (2017).
55. Walker, A. P. et al. The impact of alternative trait-scaling hypotheses for the maximum photosynthetic carboxylation rate (V_{cmax}) on global gross primary production. *New Phytol*. **215**, 1370–1386 (2017).
56. Kato, E., Kinoshita, T., Ito, A., Kawamiya, M. & Yamagata, Y. Evaluation of spatially explicit emission scenario of land-use change and biomass burning using a process-based biogeochemical model. *J. Land Use Sci*. **8**, 104–122 (2013).
57. Tang, Z. et al. Patterns of plant carbon, nitrogen, and phosphorus concentration in relation to productivity in China's terrestrial ecosystems. *Proc. Natl Acad. Sci. USA* **115**, 4033–4038 (2018).
58. Poorter, H. et al. Biomass allocation to leaves, stems and roots: meta-analyses of interspecific variation and environmental control. *New Phytol*. **193**, 30–50 (2012).
59. Heldal, M., Norland, S. & Tumyr, O. X-ray microanalytic method for measurement of dry matter and elemental content of individual bacteria. *Appl. Environ. Microbiol*. **50**, 1251–1257 (1985).
60. von Stockar, U. & Liu, J. Does microbial life always feed on negative entropy? Thermodynamic analysis of microbial growth. *Biochim. Biophys. Acta* **1412**, 191–211 (1999).
61. Guo, L., Lin, H., Fan, B., Cui, X. & Chen, J. Impact of root water content on root biomass estimation using ground penetrating radar: evidence from forward simulations and field controlled experiments. *Plant Soil* **371**, 503–520 (2013).
62. Glass, S. V. & Zelinka, S. L. in *Wood Handbook: Wood as an Engineering Material* Vol. 190, 4.1–4.19 (US Department of Agriculture, 2010).
63. Loveys, B. R. et al. Thermal acclimation of leaf and root respiration: an investigation comparing inherently fast- and slow-growing plant species. *Glob. Change Biol*. **9**, 895–910 (2003).
64. Sheremetev, S. N. *Herbs on the Soil Moisture Gradient (Water Relations and the Structural-Functional Organization)* (KMK, 2005).
65. Michaletz, S. T. & Johnson, E. A. A heat transfer model of crown scorch in forest fires. *Can. J. For. Res*. **36**, 2839–2851 (2006).
66. Messier, J., McGill, B. J. & Lechowicz, M. J. How do traits vary across ecological scales? A case for trait-based ecology. *Ecol. Lett*. **13**, 838–848 (2010).
67. Boucher, F. C., Thuiller, W., Arnoldi, C., Albert, C. H. & Lavergne, S. Unravelling the architecture of functional variability in wild populations of *Polygonum viviparum* L. *Funct. Ecol*. **27**, 382–391 (2013).
68. Dahlin, K. M., Asner, G. P. & Field, C. B. Environmental and community controls on plant canopy chemistry in a Mediterranean-type ecosystem. *Proc. Natl Acad. Sci. USA* **110**, 6895–6900 (2013).
69. Kattge, J. et al. TRY–a global database of plant traits. *Glob. Change Biol*. **17**, 2905–2935 (2011).
70. Lebigot, E. O. Uncertainties: a Python package for calculations with uncertainties. https://pythonhosted.org/uncertainties/ (2010).
71. Wiedenhofer, D., Fishman, T., Lauk, C., Haas, W. & Krausmann, F. Integrating material stock dynamics into economy-wide material flow accounting: concepts, modelling, and global application for 1900–2050. *Ecol. Econ*. **156**, 121–133 (2019).

Acknowledgements We thank U. Alon, S. Dan, G. Eshel, T. Fishman, E. Gelbrieth, T. Kaufmann, T. Klein, A. Knoll, E. Noor, N. Page, R. Phillips, J. Pongratz, M. Shamir, M. Shtein, B. Smith, C. Waters, T. Wiesel, M. Williams and members of our laboratory for help and discussions, and S. Sitch and the TRENDY DGVM community for access to their simulation outputs. This research was supported by the European Research Council (Project NOVCARBFIX 646827); Beck-Canadian Center for Alternative Energy Research; Dana and Yossie Hollander; Ullmann Family Foundation; Helmsley Charitable Foundation; Larson Charitable Foundation; Wolfson Family Charitable Trust; Charles Rothschild; and Selmo Nussenbaum. R.M. is the Charles and Louise Gartner professional chair. Y.M.B.-O is an Azrieli Fellow.

Author contributions E.E., L.B.-U. and R.M. wrote the manuscript. E.E. performed the bulk of the research and data analysis. L.B.-U. contributed to the anthropogenic mass analysis and biomass estimation. Y.M.B.-O. contributed to the biomass estimation and carbon content calculation. J.G. contributed to the water content calculation. E.E., J.G. and Y.M.B.-O. performed the uncertainty analysis. E.E., L.B.-U. and R.M. conceived the study. R.M. supervised the study. All authors discussed the results, and commented on the manuscript.

Competing interests The authors declare no competing interests.

Additional information

Supplementary information is available for this paper at https://doi.org/10.1038/s41586-020-3010-5.

Correspondence and requests for materials should be addressed to R.M.

Peer review information *Nature* thanks Fridolin Krausmann, Dominik Wiedenhofer and the other, anonymous, reviewer(s) for their contribution to the peer review of this work.

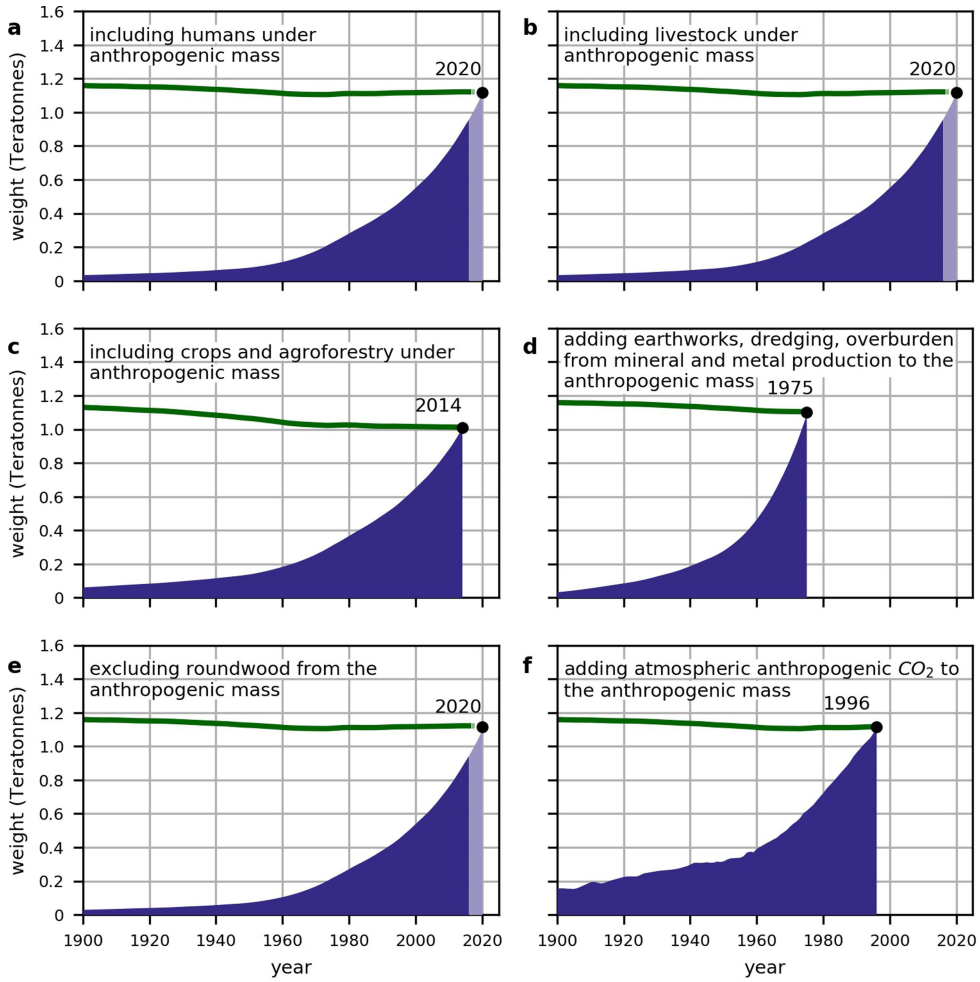

Extended Data Fig. 1 | Sensitivity analysis of the anthropogenic mass definition. a–**f**, The effect of adding the following to the anthropogenic mass (dark purple): **a**, mass of the human population, **b**, mass of livestock, **c**, mass of crops and agroforestry, **d**, mass of earthworks, dredging and waste/overburden from mineral and metal production, and **f**, mass of anthropogenic atmospheric CO_2 stocks, as well as **e**, the exclusion of the mass of industrial roundwood. The total biomass weight is depicted by the green line. Black dot indicates the year of intersection based on the alternative anthropogenic mass definition. Violet area and light green-dashed line indicate extrapolated anthropogenic mass and biomass estimates, respectively. Full description of the sensitivity analysis is provided in Supplementary Information section 1.

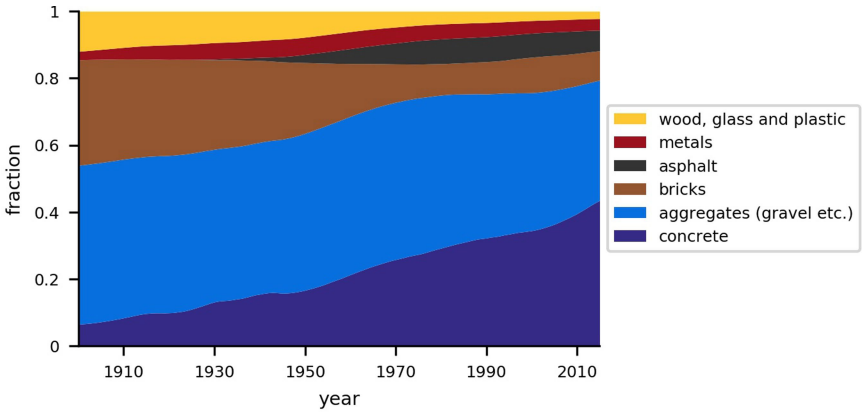

Extended Data Fig. 2 | Anthropogenic mass composition since the year 1900, divided into material groups. Dataset is based on ref. [22].

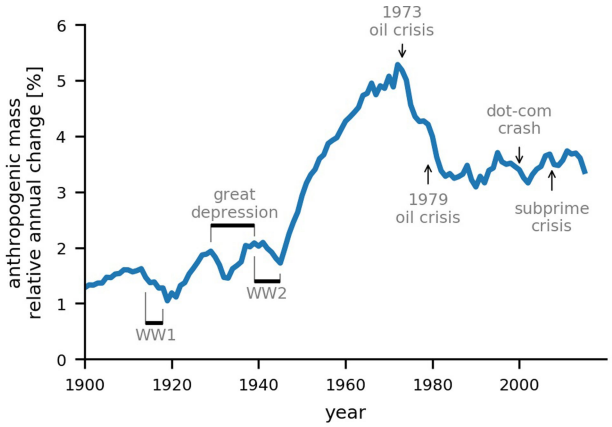

Extended Data Fig. 3 | Anthropogenic mass relative annual change, with highlights of notable global events. Relative annual change is calculated as the difference between two consecutive years divided by the earlier year anthropogenic mass value.

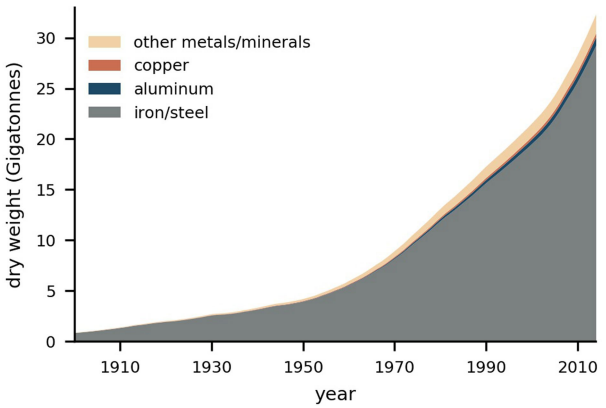

Extended Data Fig. 4 | Anthropogenic mass metal estimates since the beginning of the twentieth century, divided into material sub-groups. Data are taken from the comprehensive work of the Institute of Social Ecology, Vienna. We used a recent study[71], which has some minor updates compared to the study used to achieve the main results[22].

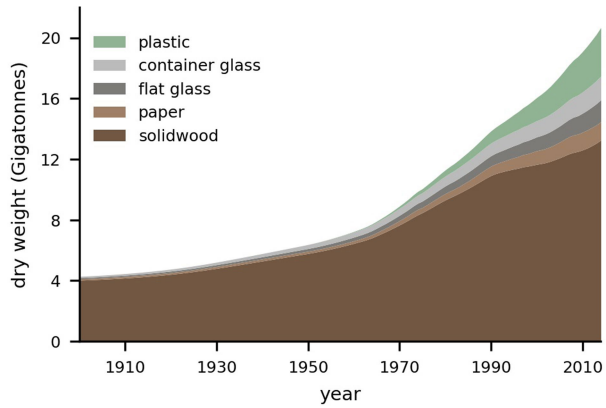

Extended Data Fig. 5 | Anthropogenic mass estimates for (industrial round) wood, glass and plastic since the beginning of the twentieth century, divided into material sub-groups. Data are taken from the comprehensive work of the Institute of Social Ecology, Vienna. We used a recent study[71], which has some minor updates compared to the study used to achieve the main results[22].

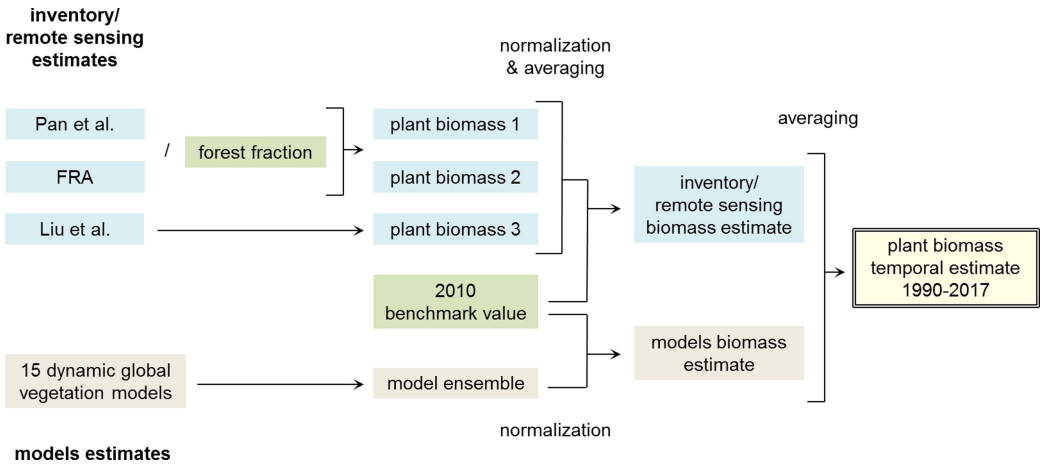

Extended Data Fig. 6 | Calculation steps in plant biomass estimation for 1990–2017. As further detailed in the Methods section 'Biomass change over the years 1900–2017'.

Extended Data Table 1 | The different anthropogenic mass groups and their mass estimates in selected years

Anthropogenic mass group	Description	1900	1940	1980	2020
concrete	Used mostly for building and infrastructure construction. Comprises a mix of materials, including cement and aggregates (gravel and sand).	2	10	86	549
aggregates	Gravel and sand, mainly used as bedding for roads and buildings. Aggregates used for production of concrete and asphalt are accounted under those categories and not here.	17	30	135	386
bricks	Mostly composed of clay and used for constructions.	11	16	28	92
asphalt	Composed of bitumen and aggregates (gravel and sand), used mainly for road construction/pavement.	0	1	22	65
metals	Mostly iron/steel, aluminum and copper.	1	3	13	39
other	Including industrial roundwood, in the form of solidwood products and paper/paperboard, container and flat glass and plastic.	4	6	11	23

The mass values are presented in gigatonnes (Gt; 1,000 Gt = 1 Tt). The 2020 estimate is partially extrapolated (since 2016). Overall, the categories of anthropogenic mass presented give almost complete coverage of materials usage (>98% in terms of mass based on ref. [21]).

nature research

Corresponding author(s): Ron Milo

Last updated by author(s): Sep 5, 2020

Reporting Summary

Nature Research wishes to improve the reproducibility of the work that we publish. This form provides structure for consistency and transparency in reporting. For further information on Nature Research policies, see Authors & Referees and the Editorial Policy Checklist.

Statistics

For all statistical analyses, confirm that the following items are present in the figure legend, table legend, main text, or Methods section.

n/a	Confirmed	
☐	☒	The exact sample size (*n*) for each experimental group/condition, given as a discrete number and unit of measurement
☒	☐	A statement on whether measurements were taken from distinct samples or whether the same sample was measured repeatedly
☒	☐	The statistical test(s) used AND whether they are one- or two-sided *Only common tests should be described solely by name; describe more complex techniques in the Methods section.*
☒	☐	A description of all covariates tested
☒	☐	A description of any assumptions or corrections, such as tests of normality and adjustment for multiple comparisons
☐	☒	A full description of the statistical parameters including central tendency (e.g. means) or other basic estimates (e.g. regression coefficient) AND variation (e.g. standard deviation) or associated estimates of uncertainty (e.g. confidence intervals)
☒	☐	For null hypothesis testing, the test statistic (e.g. *F*, *t*, *r*) with confidence intervals, effect sizes, degrees of freedom and *P* value noted *Give P values as exact values whenever suitable.*
☐	☒	For Bayesian analysis, information on the choice of priors and Markov chain Monte Carlo settings
☒	☐	For hierarchical and complex designs, identification of the appropriate level for tests and full reporting of outcomes
☒	☐	Estimates of effect sizes (e.g. Cohen's *d*, Pearson's *r*), indicating how they were calculated

Our web collection on statistics for biologists contains articles on many of the points above.

Software and code

Policy information about availability of computer code

Data collection	All code used in this study is available on GitHub, at https://github.com/milo-lab/anthropogenic_mass.
Data analysis	All code used in this study is available on GitHub, at https://github.com/milo-lab/anthropogenic_mass.

For manuscripts utilizing custom algorithms or software that are central to the research but not yet described in published literature, software must be made available to editors/reviewers. We strongly encourage code deposition in a community repository (e.g. GitHub). See the Nature Research guidelines for submitting code & software for further information.

Data

Policy information about availability of data

All manuscripts must include a data availability statement. This statement should provide the following information, where applicable:

- Accession codes, unique identifiers, or web links for publicly available datasets
- A list of figures that have associated raw data
- A description of any restrictions on data availability

All data used in this study are available on GitHub, at https://github.com/milo-lab/anthropogenic_mass. Anthropogenic mass data is available from ref. 22 and at: https://boku.ac.at/wiso/sec/data-download. TRENDY Dynamic Global Vegetation Models outputs are available at: https://sites.exeter.ac.uk/trendy. Leaves dry matter content measurements were obtained via TryDB, at: https://www.try-db.org/. Other datasets used in this study are available from published literature, as detailed in the Methods section and Supplementary Information.

Field-specific reporting

Please select the one below that is the best fit for your research. If you are not sure, read the appropriate sections before making your selection.

☐ Life sciences ☐ Behavioural & social sciences ☒ Ecological, evolutionary & environmental sciences

For a reference copy of the document with all sections, see nature.com/documents/nr-reporting-summary-flat.pdf

Ecological, evolutionary & environmental sciences study design

All studies must disclose on these points even when the disclosure is negative.

Study description	Quantitative comparison of the global living biomass and human-made mass, since the beginning of the 20th century.
Research sample	Human-made mass data, divided into material sub-groups and living biomass data.
Sampling strategy	All relevant data were used. No statistical methods were used to predetermine sample size.
Data collection	Data was based on existing datasets and was collected online by the authors.
Timing and spatial scale	Global data since 1900, consistent with the time period and global scope of the study.
Data exclusions	No data were excluded from the analyses.
Reproducibility	This is not an experimental study, thus experimental replication was not performed. The analysis is reproducible given the code provided, which includes all steps from raw data to end results.
Randomization	All living organisms were grouped into one group, all human-made masses were grouped into another group.
Blinding	Not relevant, since this study is not experimental.

Did the study involve field work? ☐ Yes ☒ No

Reporting for specific materials, systems and methods

We require information from authors about some types of materials, experimental systems and methods used in many studies. Here, indicate whether each material, system or method listed is relevant to your study. If you are not sure if a list item applies to your research, read the appropriate section before selecting a response.

Materials & experimental systems

n/a	Involved in the study
☒	☐ Antibodies
☒	☐ Eukaryotic cell lines
☒	☐ Palaeontology
☒	☐ Animals and other organisms
☒	☐ Human research participants
☒	☐ Clinical data

Methods

n/a	Involved in the study
☒	☐ ChIP-seq
☒	☐ Flow cytometry
☒	☐ MRI-based neuroimaging